

Significant enhancement of the electrical transport properties of graphene films by controlling the surface roughness of Cu foils before and during chemical vapor deposition.

Dongmok Lee,^{a,b} Gi Duk Kwon,^b Jung Ho Kim,^{a,b} Eric Moyen,^b Young Hee Lee,^{a,b,c} Seunghyun Baik^{*a,d} and Didier Pribat.^{*b}

^a Center for Integrated Nanostructure Physics, Institute for Basic Science (IBS), Suwon 440-746, Republic of Korea.

^b Department of Energy Science, Sungkyunkwan University, Suwon 440-746, Republic of Korea.

^c Department of Physics, Sungkyunkwan University, Suwon 440-746, Republic of Korea.

^d School of Mechanical Engineering and Samsung-SKKU Graphene Center (SSGC), Sungkyunkwan University, Suwon 440-746, Republic of Korea.

Corresponding Authors

* Prof. D. Pribat, didier53@skku.edu

* Prof. S. Baik, sbaik@me.skku.ac.kr

Supporting information

The developed AFM profile lengths have been evaluated by numerically integrating the measured profiles according to the following equation:

$$L = \int_0^{50} \sqrt{1 + f'(x)^2} dx,$$

where $f'(x)$ is the numerical derivative of the function representing the profile and x is in μm . A central difference algorithm and a trapezoidal algorithm have been used for, respectively, numerical integration and differentiation.

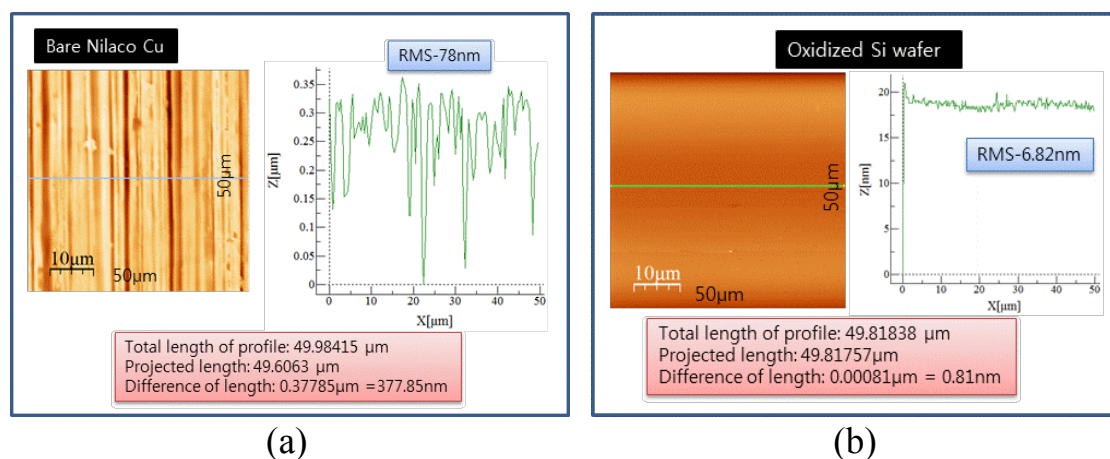


Figure S1. Measurements of AFM profile lengths on a raw Nilaco Cu foil (a) and an oxidized Si substrate (b). The length difference is ~ 377 nm over a projected distance of $50 \mu\text{m}$.

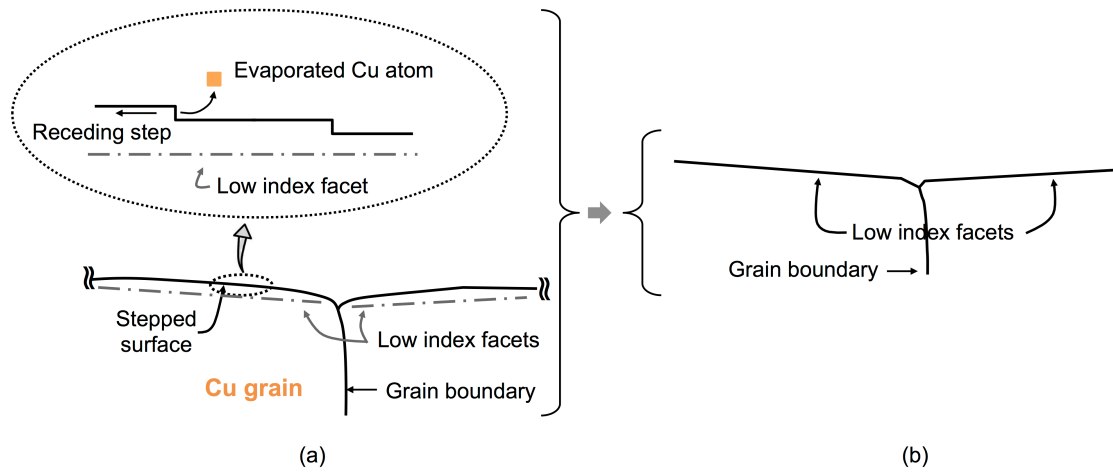


Figure S2. Schematics of the evaporation-induced planarization effect taking place during high temperature annealing of Cu foils. (a) The starting Cu surface with the inset on top showing the receding of surface steps upon evaporation of Cu atoms from the surface. (b) The ideal surface obtained after a long annealing. Low index facets have been formed, including at the emergence of the grain boundary.

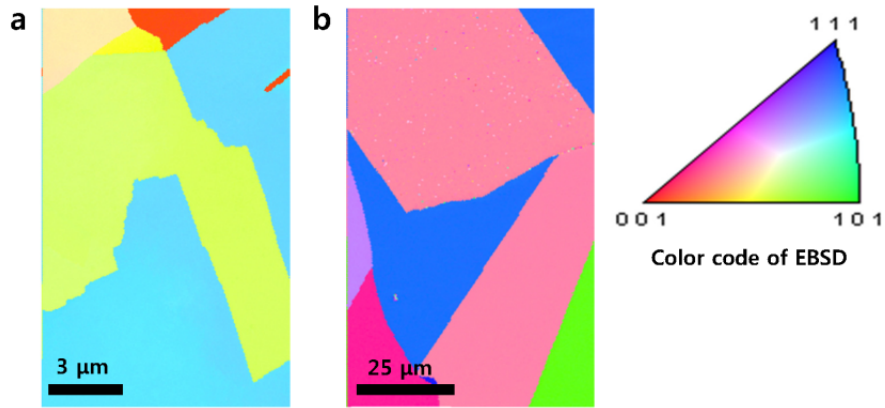


Figure S3. The electron backscattering diffraction (EBSD) analysis of a polycrystalline Cu substrate before (a) and after (b) the annealing process at 1050 °C. The surface of the Cu substrate was pre-electropolished for better imaging. The scale bars in (a) and (b) are 3 and 25 μm, respectively. Note the significant increase in grain size following high temperature annealing.

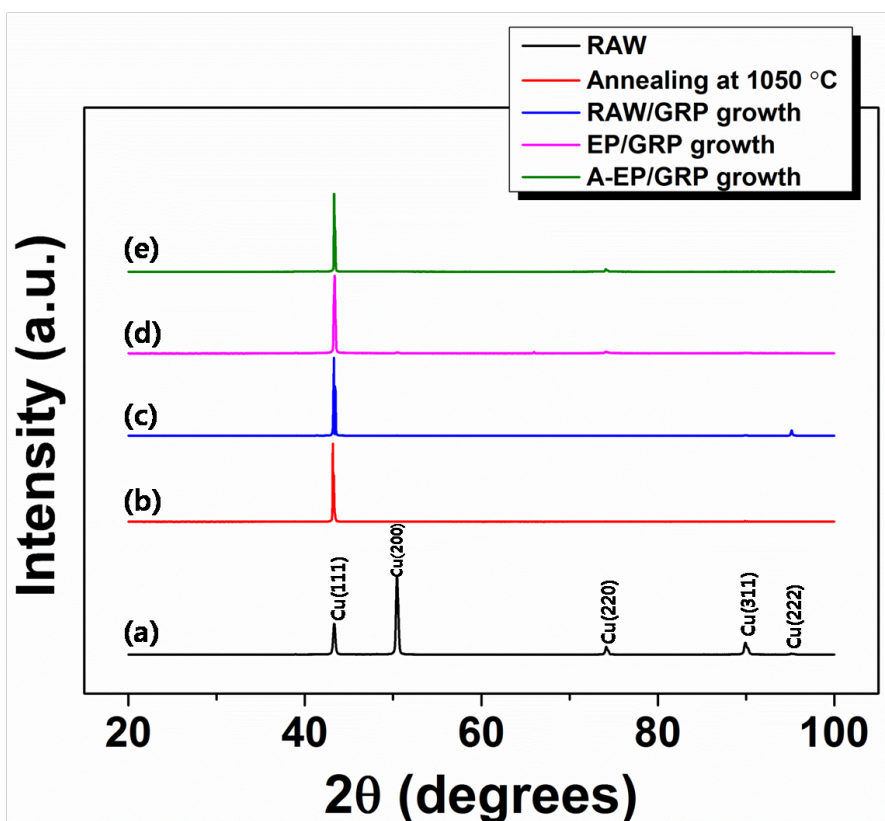


Figure S4: X-ray diffraction spectra recorded on Cu foils after various treatments. (a) as received RAW substrate; (b) after annealing at 1050°C of the RAW substrate; (c) after graphene growth on a RAW substrate; (d) after graphene growth on an EP substrate; (e) after graphene growth on an A-EP substrate.

Although the as-received RAW substrates exhibit various grain orientations, the (200) peak is the strongest, corresponding to a (100) texture, induced by the cold rolling process which is used to manufacture the Cu foils^a. After annealing at 1000 °C (remember that graphene growth includes first a 1000 °C annealing step during 30 minutes) or 1050 °C, the texture changes to (111) for all samples. The xrd measurements were performed at approximately the same location on the Cu foil for the RAW, A-EP and A-EP + graphene growth sample.

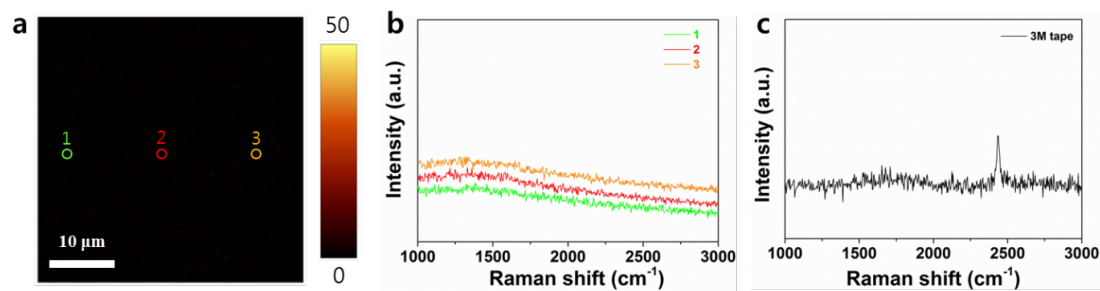


Figure S5. (a) Raman mapping of the Cu surface after removing graphene using 3M scotch tape. (b) Raman spectra corresponding to the 3 different spots shown on (a). (c) Raman spectrum of a 3M scotch tape (as received).

As shown in Figure S5c, a characteristic peak of the 3M scotch tape was observed at $\sim 2440 \text{ cm}^{-1}$ which we attributed to P-H bonding^b. As shown in (a) and (b), neither this peak, nor any graphene-related one were found after peeling off the Cu substrate. This indicates that (i), graphene was successfully removed from the Cu surface and (ii) no scotch residues were left on the Cu surface.

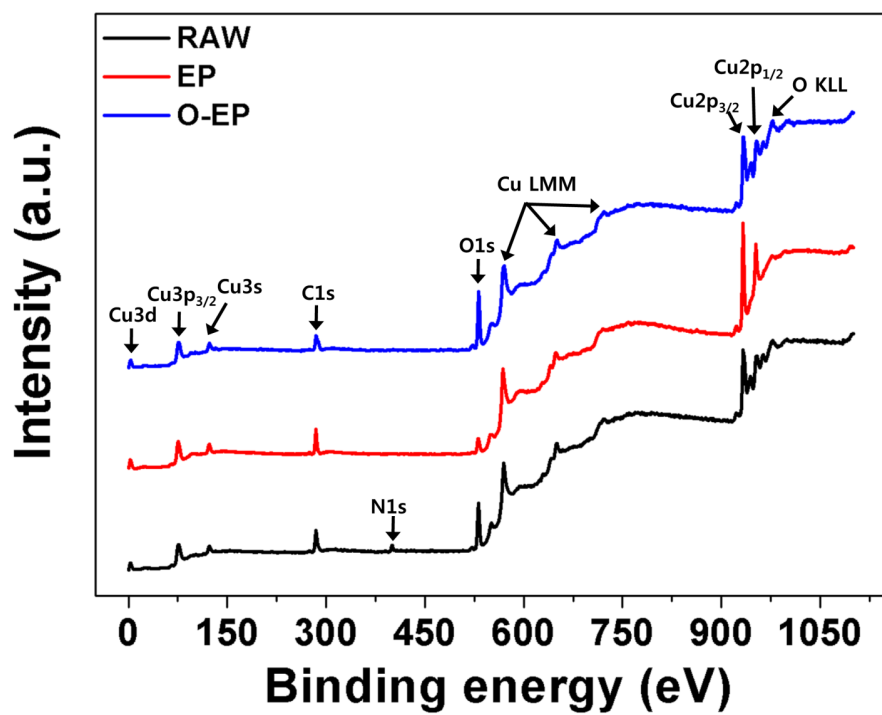


Figure S6. The XPS spectra of RAW, EP, and O-EP samples. The Cu2p_{3/2}, Cu2p_{1/2}, and CuO modes between 930 and 960 eV are magnified in Figure 2c.

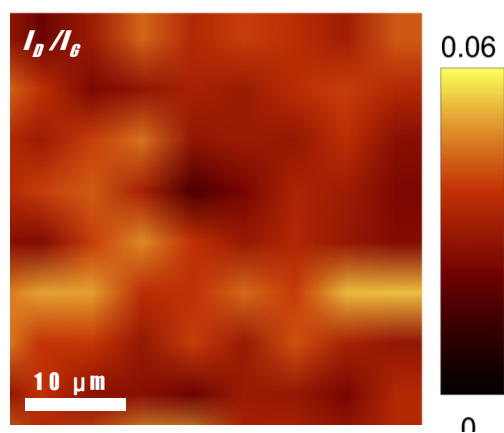


Figure S7. The Raman area map of the D-to-G mode intensity ratio of A-EP sample (10 x 10 pixels). The intensity ratio was smaller than 0.06 demonstrating a uniform high crystalline quality graphene. The excitation wavelength was 532 nm.

Evaluation of the sheet resistance variation as a function of grain size

We evaluated the sheet resistance variation as a function of the average grain size, using the formula derived by Tsen *et al.* (Ref. 15 of the paper). When we measure the sheet resistance with the 4 point probe technique, we are in the situation corresponding to $L \gg D$, where L is the length of the device (ie the distance between probes, which is 1 mm) and D is the average grain size (1~4 μm in our work). In this configuration, the sheet resistance of the graphene (Rs) is given by¹⁵: $Rs \approx \rho_{sq} \left(1 + \lambda/D\right)$, where ρ_{sq} is the single domain sheet resistance (without the grain boundary effect) and λ represents the grain boundary connectivity. λ depends upon the growth process used for graphene synthesis (as well as the grain size) and in Ref. 15, the values of λ were ~ 110 nm for a growth type similar to ours (grain size in the 1 μm range, rapid coverage of the Cu substrate) and 880 nm for a growth type yielding large grains (50 μm and more).

Hence, for the EP samples, where the grain size is ~ 2.8 μm (see Figures 4b & e):

$$Rs_{EP} \approx \rho_{sq} \left(1 + 110/2800\right) \approx \rho_{sq} \times 1.04.$$

Now, for the A-EP sample, with a 3.5 μm grain size (see Figures 4d & e):

$$Rs_{A-EP} \approx \rho_{sq} \left(1 + 110/3500\right) \approx \rho_{sq} \times 1.0314.$$

We assumed that the values of λ and ρ_{sq} were the same for the EP and A-EP samples, since the growth conditions were exactly the same, only the substrate roughness was different. Therefore, the ratio of Rs_{EP}/Rs_{A-EP} was 1.0083, whereas experimentally we found $306/209.9 \approx 1.4578$ (see the exact values of sheet resistance in Table S1 below, corresponding to Figure 3c).

This means that the grain size variation alone cannot account for the variation in sheet resistance that we have measured. Note that if instead of $\lambda \approx 110$ nm, we take $\lambda \approx 880$ nm (which does not correspond to the physical situation we observe, but would be an extreme case) we get $Rs_{EP}/Rs_{A-EP} \approx 1.05$, which again is far from 1.4578. Even $\lambda \approx 1.8$ μm (see Ref. 15) yields $Rs_{EP}/Rs_{A-EP} \approx 1.09$, again far from 1.4578.

	RMS (nm)	Rs 1(Ω/\square)	Rs 2(Ω/\square)	Rs 3(Ω/\square)	Rs _{average} (Ω/\square)	Standard Deviation
A-EP	13	202.3	214.5	213.0	209.9	6.7
EP	25	301.7	307.0	309.4	306.0	4.0
	39	338.3	337.2	337.7	337.7	0.6
	47	356.1	355.7	369.7	360.5	8.0
	56	373.7	374.2	373.4	373.8	0.4
RAW	58	549.0	541.0	566.5	552.2	13.0

Table S1 : Surface roughness values (RMS) and corresponding sheet resistance measurements (Rs) of the samples shown in Figure 3c. The standard deviation is also indicated in the last column.

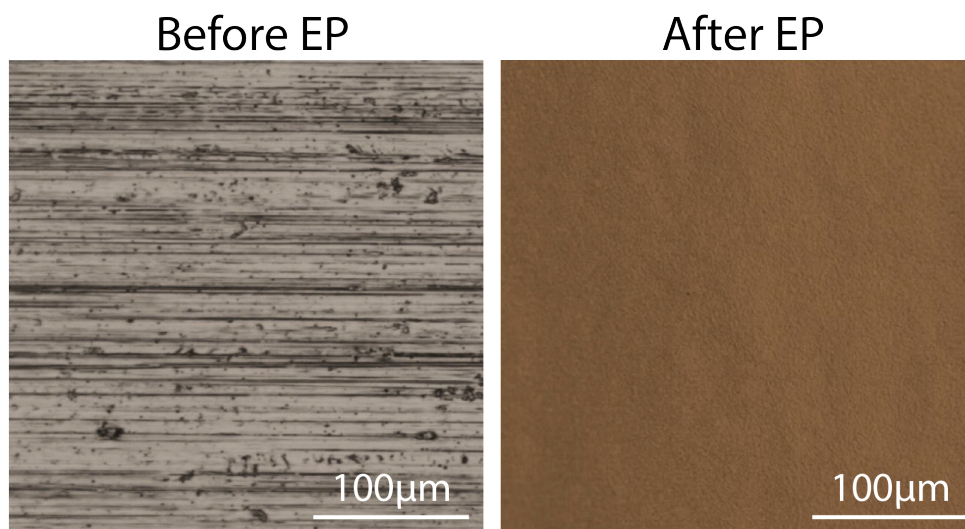


Figure S8. Optical images of a Cu foil before and after electropolishing. Any impurity lying on the surface of the Cu foil was removed during electropolishing.

Evaluation of the sheet resistance using the van der Pauw method.

The basic van der Pauw electrode configuration is illustrated on Figure S9 below.

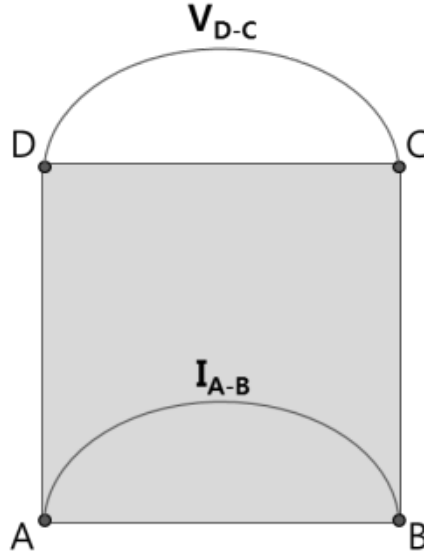


Figure S9: Schematics of the van der Pauw contact geometry.

A, B, C and D are the indium (In) contacts located at the corners of square-shaped graphene sheet (5 mm x 5 mm). We define the resistance $R_{AB,CD}$ as the potential difference $V_D - V_C$ per unit current through the contacts between A and B. Likewise, we define the resistance $R_{BC,DA}$. Then, the sheet resistance (R_{sh}) was calculated using the following equations (1) and (2)^c:

$$R_{sh} = \frac{\pi}{\ln 2} \frac{(R_{AB,CD} + R_{BC,DA})}{2} f \left(\frac{R_{AB,CD} - R_{BC,DA}}{R_{AB,CD} + R_{BC,DA}} \right) \quad (1)$$

$$f \approx 1 - \left(\frac{R_{AB,CD} - R_{BC,DA}}{R_{AB,CD} + R_{BC,DA}} \right)^2 \frac{\ln 2}{2} - \left(\frac{R_{AB,CD} - R_{BC,DA}}{R_{AB,CD} + R_{BC,DA}} \right)^4 \left\{ \frac{(\ln 2)^2}{4} - \frac{(\ln 2)^3}{12} \right\} \quad (2)$$

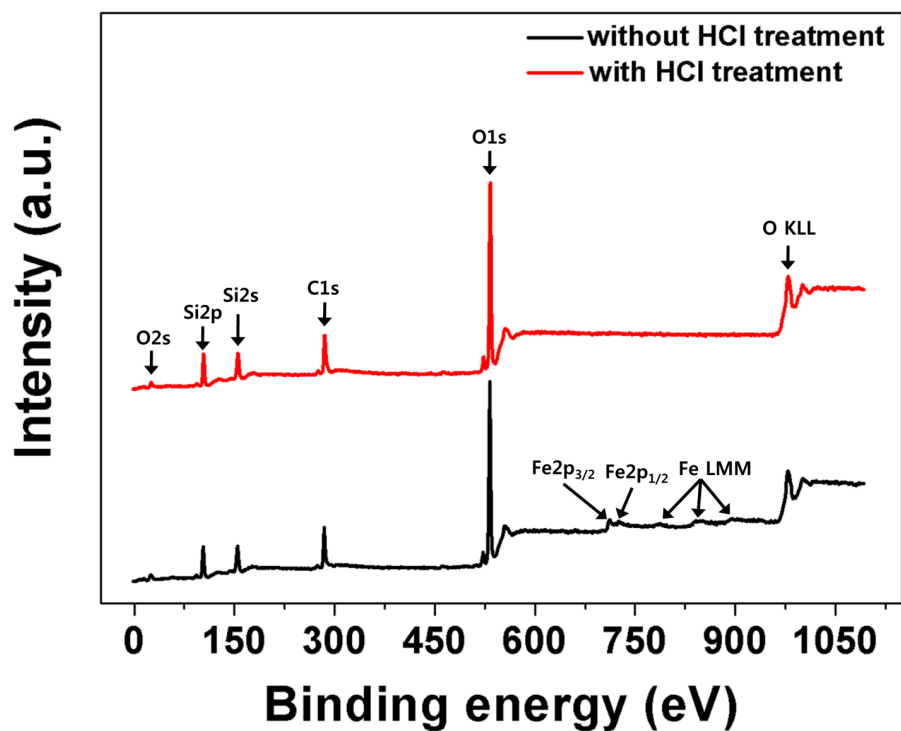


Figure S10. The XPS spectra of graphene transferred on SiO₂/Si substrates with and without HCl treatment. The iron nanoparticle residues were removed by the HCl treatment (0.5 M, 10 min) decreasing sheet resistance. The graphene was thoroughly rinsed using de-ionized water for 2 hours after the HCl treatment.

References

- a- C.S. Barrett and T.B. Massalski, *Structure of Metals*, McGraw-Hill, Elmsford, NY, 1980.
- b- I. K. Shakirov, A. R. Safiullin, R. R. Shagidullin, A. M. Polozov, and O. N. Nuretdinova, *Russian Chem. Bull.* 1992, **41**, 2158.
- c- L. J. van der Pauw, *Philips Tech. Rev.* 1958, **20**, 220.